Daniel Bugelnig, Mireia López

Case Study: La Palma Vulcano Eruption

Project Report

AI4EO

UPC

Escola Tècnica Superior d'Enginyeria de Telecomunicació de Barcelona
UNIVERSITAT POLITÈCNICA DE CATALUNYA
BARCELONATECH

Evaluator and Supervisor: López Martinez Carlos

Barcelona, June 2025

Contents

List of Figures

List of Tables

Chapter 1

Introduction

What has happened in the area?

In 2021, the island of La Palma, one of the Canary Islands, experienced a significant volcanic eruption. The eruption of the Cumbre Vieja volcano on La Palma began on 19 September 2021 and lasted nearly three months, marking it as one of the most destructive eruptions in the island's history. The eruption resulted in lava flows that covered buildings, agricultural land, and infrastructure. It also led to the evacuation of thousands of people and destroyed over 1100 buildings and around 500 hectares of land. Volcanic activity continued for several weeks, accompanied by seismic events and temporary airport closures due to ash.[1]
Figure 1.1 shows the location of the event.

Figure 1.1: La Palma while the ongoing eruption[1]

To further evaluate the extent and impact of the disaster, we use AI-based tools for change detection and land cover prediction.

- Comparing pre- and post-eruption satellite images using calculated indices.
- Selecting the most significant indices
- Training AI models using these selected indices to classify land cover and detect changes.

Chapter 2

Data Overview

2.1 What data is being used for the analysis?

The analysis focuses on the natural disaster scenario of the **La Palma volcano eruption (2021)**. To investigate the environmental impact of the eruption, we utilize multisensor satellite data from open-access platforms provided by the European Space Agency (ESA) and Copernicus. The dataset includes optical and radar imagery from Sentinel-1 and Sentinel-2, as well as a thematic land cover layer.

The following table summarizes the data sources used:

- **Sentinel-1 (GRD)**:
  - **Acquisition Dates**: 2021-08-23 and 2022-01-08
  - **Polarizations**: VV and VH
- **Sentinel-2 (L2A)**:
  - **Acquisition Dates**: 2021-08-26 and 2022-01-03
  - **Tile ID**: 28RBS
  - **Bands Used**: B2 - B12
  - **Resolution**: 10 m
- **Land Cover Layer**:
  - **Year**: 2021

The combined use of Sentinel-1 radar and Sentinel-2 optical imagery provides a robust dataset for analyzing both physical changes and environmental impacts of the volcanic eruption.

2.2 Information obtained through the acquired data

To gain more information from the obtained data, we compute several indices to improve the analysis. These indices are listed in 2.1

Index Name	**Formula**
	Sentinel-1 Indices
Amplitude (VV, VH)	$A = \sqrt{DN}$
VH/VV Ratio	$\text{Ratio} = \frac{\sigma^0_{VH}}{\sigma^0_{VV}}$
Sigma Nought (σ°)	$\sigma^0 = 10\log_{10}(DN^2) - A$
RVI	$RVI = \frac{4\times\sigma^0_{VH}}{\sigma^0_{VV}+\sigma^0_{VH}}$
RWI	$RWI = \frac{\sigma^0_{VH}}{\sigma^0_{VV}+\sigma^0_{VH}}$
MPDI	$MPDI = \frac{\sigma^0_{VV}-\sigma^0_{HH}}{\sigma^0_{VV}+\sigma^0_{HH}}$
	Sentinel-2 Indices
NDVI	$NDVI = \frac{B8-B4}{B8+B4}$
NDWI	$NDWI = \frac{B3-B8}{B3+B8}$
AWEI	$AWEI = 4 \times (B3 - B11) - (0.25 \times B8 + 2.75 \times B12)$
NDBI	$NDBI = \frac{B11-B8}{B11+B8}$
NDSI	$NDSI = \frac{B11-B12}{B11+B12}$
NBR	$NBR = \frac{B8-B12}{B8+B12}$
NDSI	$NDSI = \frac{B3-B11}{B3+B11}$

Figure 2.1: Indices

2.2.1 Radar Indices

- **Sigma Nought (Linear)**: Represents the radar backscatter intensity in linear scale. Useful for quantifying surface roughness and moisture.
- **Sigma Nought (Logarithmic)**: The backscatter intensity expressed in decibels (dB), which is commonly used for radar analysis due to its dynamic range.
- **VH/VV Ratio**: Describes the ratio between cross-polarized (VH) and co-polarized (VV) radar returns. Helps assess surface properties and structure.
- **Radar Vegetation Index (RVI)**: Indicates how evenly radar energy is scattered. Higher values suggest denser or healthier vegetation.
- **Radar Water Index (RWI)**: Highlights areas with high moisture or water content. Useful for detecting water bodies or flooded zones.
- **Modified Polarization Difference Index (MPDI)**: Measures the difference between VV and VH signals. High values often point to urban or dry areas; low or negative values suggest vegetation or moisture.

2.2.2 Optical Indices

- **Normalized Difference Vegetation Index (NDVI)**: Measures vegetation health and density using near-infrared and red light reflectance.
- **Normalized Difference Water Index (NDWI)**: Detects surface water by comparing green and near-infrared reflectance.

- **Automated Water Extraction Index (AWEI)**: Enhances water detection in complex environments such as shadows or urban areas.
- **Normalized Difference Built-up Index (NDBI)**: Identifies urban or built-up areas by leveraging differences between SWIR and NIR reflectance.
- **Normalized Difference Snow Index (NDSI, SWIR version)**: Detects snow by comparing two shortwave infrared bands.
- **Normalized Difference Snow Index (Green–SWIR version)**: An alternative snow detection index using green and SWIR bands.
- **Normalized Burn Ratio (NBR)**: Assesses fire damage or burned vegetation. Lower values indicate burned areas.

We use these indices because they support our analysis, and they give us more insight into these pictures. We also included in our study additional information, i.e., land masks for land cover and for land change. This is used for training the models to classify land cover and for detecting change.

2.2.3 Visualization of Index Calculations

For a complete overview, all indices are visualized in the appendix. Below, a small selection is displayed (Figures 2.2, 2.3, 2.5, 2.4).

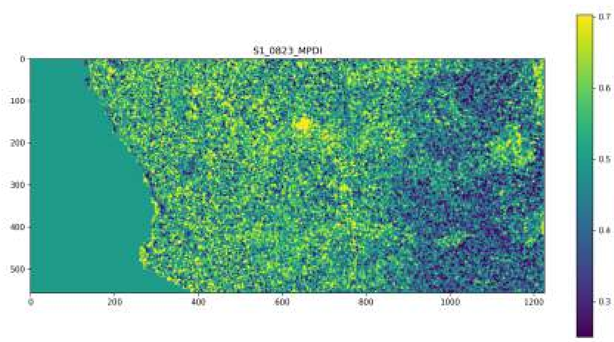

Figure 2.2: MPDI of S1, captured on 23.08.2021

2.3 Is there any other data missing?

Additional indices specifically for volcanic analysis would be valuable to include, as they could provide more targeted insights into thermal activity, ash dispersion, and surface changes related to volcanic processes. Moreover, higher spatial resolution data would enhance the precision and reliability of the derived indices.

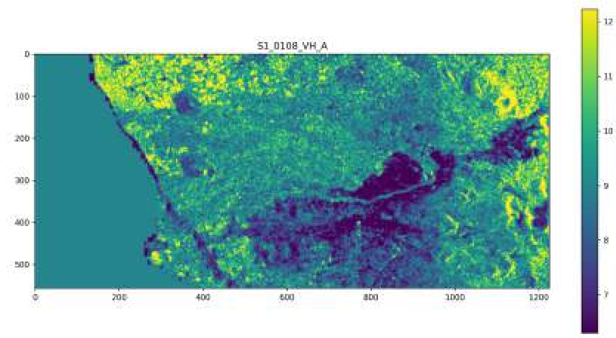

Figure 2.3: VH of S1, captured on 08.01.2022

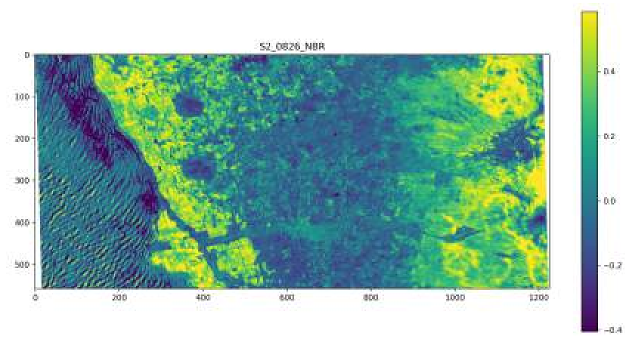

Figure 2.4: NBR of S2, captured on 26.08.2021

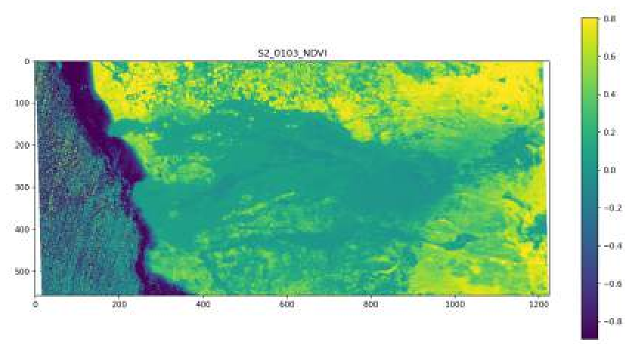

Figure 2.5: NDVI of S2, captured on 03.01.2022

Chapter 3

Preliminary Data Analysis

3.1 What has happened in the area?

La Palma is a 47-kilometer-long island in the Canary Islands. It has two main volcanic areas. The older northern part has a large crater called Caldera Taburiente, which was formed after parts of the volcano collapsed. The southern part, called Cumbre Vieja, is younger and more active. It started forming about 125,000 years ago and has had many eruptions in the last 7,000 years. These eruptions created many small craters and lava flows that run down to the sea.

Since the 15th century, there have been several eruptions that caused small explosions and lava flows, sometimes damaging homes and towns. Lava reached the ocean in the years 1585, 1646, 1677–78, 1712, 1949, 1971. After several years of increased earthquake activity, two cracks opened in the ground, and many vents released lava fountains, ash clouds, and lava flows, starting the last volcanic eruption on 19 September 2021[2], it lasted for 85 days, ending in December of that same year[3]. The island's steep terrain, dense population in certain valleys, and economic dependence on agriculture and tourism increase its vulnerability to volcanic and seismic events. La Palma also lacks large-scale evacuation infrastructure, making such disasters particularly disruptive. Although Spain has robust civil protection agencies, the remoteness of La Palma meant logistical challenges in evacuations and relief. Around 7,000 people had to be evacuated, and over 3,000 buildings were destroyed or damaged. The numbers could be resumed [4]:

- Total area covered by lava flows: about 12.2 km^2 (1,219 hectares)
- Buildings destroyed: Over 3,000 structures
- Roads buried or damaged: Over 73 km
- Farms and greenhouses: Hundreds damaged (especially banana plantations)
- Evacuated population: Approximately 7,000 people had to evacuate, mostly from:
  - El Paso
  - Los Llanos de Aridane
  - Tazacorte
  - Todoque (completely buried)

3.2 Which area appears to be affected?

The affected area is located on the western part of La Palma. The impacted region spans several square kilometers and includes urban zones, farmlands, and forested terrain. Optical imagery from before and after the eruption highlights the transformation of land cover due to lava flooding, seen in Figure 3.1.

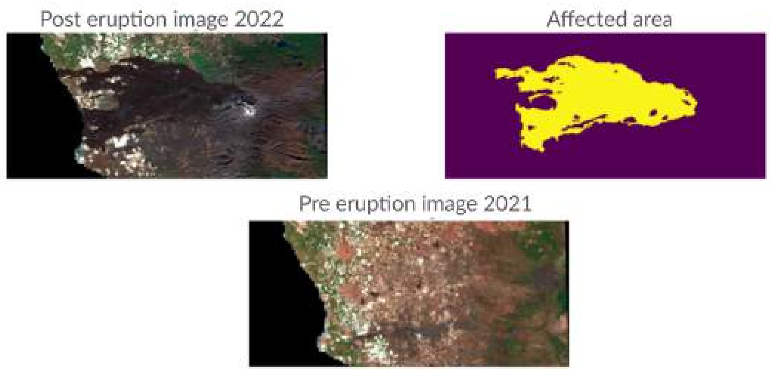

Figure 3.1: Optical RGB images before and after the eruption, including the detected affected area.

3.3 Most significantly affected aspect

The volcanic eruption caused the most serious damage to infrastructure, but this also had a strong effect on the people living there. The lava destroyed more than 3,000 buildings, including homes, farms, schools, and businesses. It also covered over 90 kilometers of roads, making many areas impossible to reach. Because of this, around 7,000 people had to leave their homes. Many lost everything and could not return to their neighborhoods. One town, Todoque, was completely buried by lava. This damage not only took away people's homes and jobs but also broke up communities. Basic services like water, electricity, and phone connections were cut off. As a result, the destruction of infrastructure made the social situation worse. People were left without shelter, income, or access to help.

3.4 Proposed next steps for further analysis

To better understand the effects of the 2021 volcanic eruption, we plan to take several next steps in our analysis.

First, we will use time-series satellite images from Sentinel-1 and Sentinel-2 to observe how the area changed over time. This will help us clearly see the spread of lava, the loss of vegetation, and changes to the coastline.

Then, we will calculate several change detection indices like NDVI (for vegetation), AWEI (for water), NBR (for burned areas), and RWI (for surface moisture). These indices will give us more detailed information about how the land was affected.

After that, we will apply classification models such as Decision Trees, Random Forest, and MLP (Multi-layer Perceptron) to automatically classify the land into affected and unaffected areas. These models are trained using both pre- and post-eruption data and can help us map the damage more accurately. We will also use deep learning models like CNN and U-Net to detect land cover changes more precisely.

Chapter 4

Changing Detection

4.1 What was the condition of the area before the event, and how does it appear after?

After obtaining different measurements from satellites, it can be obtained different indexes, combining different bands or polarizations. Automated Water Extraction Index is usually used for the detection of water surface, highlighting water and suppressing shadows, vegetation and built-up areas.

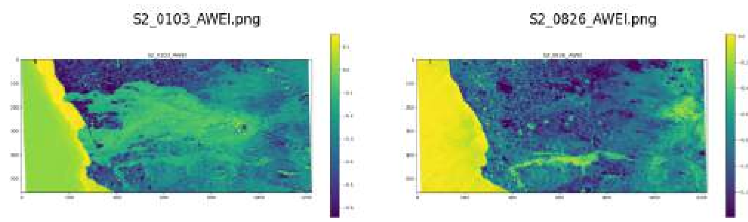

Figure 4.1: AWEI obtained images after and before the eruption, respectively

In Figure 4.1, it can be seen clearly the affected area but also the change in the coast shape, being the sea completely yellow in both images. The Normalized Difference Vegetation Index (NVDI) is used, as stated in its own name, in order to measure vegetation health and density. It compares the reflectance of NIR and red light, since healthy vegetation reflects more NIR and absorbs more red light. Values closer to 1 mean healthy and dense vegetation, values close to 0 are bare soil and negative values indicate water or non-vegetated surfaces.

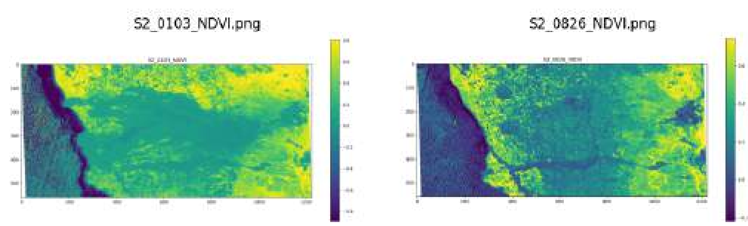

Figure 4.2: NVDI obtained images after and before the eruption, respectively

In Figure 4.2, it can be clearly seen where the affected area is located, where its value is around 0.

4.2 Compared to the preliminary evaluation, which areas are affected? Is the extent larger compared to the initial assessment?

By comparing the images of different indexes, as it is done in Figure 4.1 and in Figure 4.2, the affected area in land and the sea line changes can be easily distinguished, as it was done by comparing RGB images, as in Figure 4.3. The affected area looks similar.

Figure 4.3: RGB images after and before the eruption

4.3 Which area has undergone the most significant change due to the event?

The most significant changes can be observed in the coast line and the vegetation areas. Even if in the RGB images can be easily appreciated the difference between built up areas and the burned area, the changes in water and vegetation can be easily seen using the different indexes, due to the difference between the materials and their physical properties and reactions to the radiation of the different bands.

4.4 Do you observe anything unusual in your results? Are there any issues with the data or the outputs you are obtaining? If so, what are they and what might be the cause?

In order to detect the changed area it was used different models. The following figures correspond to MLP (Multi-layer Perceptron), Decision Tree and Random Forest, respectively. The results were quite good, as there was only a binary classification to do, nothing unusual was detected, except a bit of noise in the prediction.

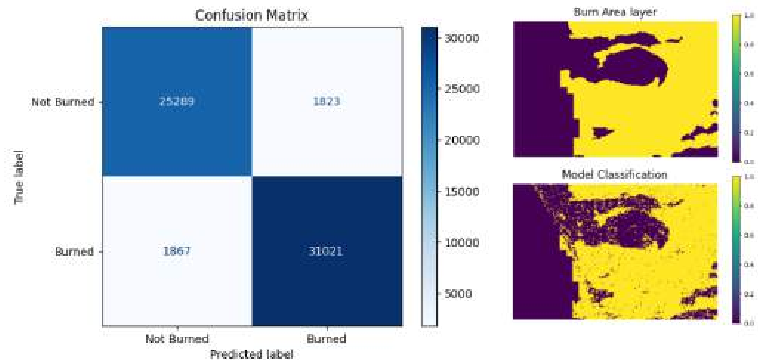

Figure 4.4: Burned area prediction using decision tree and corresponding confusion matrix

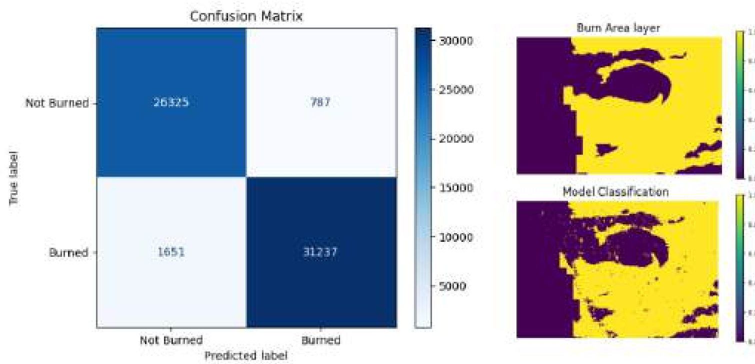

Figure 4.5: Burned area prediction using MLP and corresponding confusion matrix

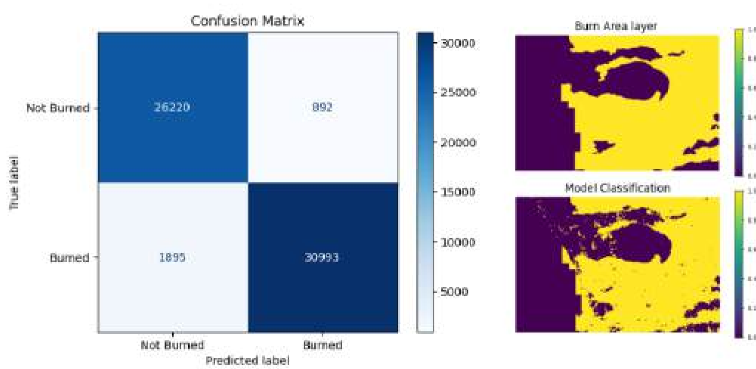

Figure 4.6: Burned area prediction using Random Forest and corresponding confusion matrix

They all showed an accuracy higher than 93%. The worse result is obtained with the decision tree model, Figure 4.4, that could be enhanced slightly by defining more strict rules, for example.

4.5 What additional analyses could be conducted to improve the understanding and comparison of the affected area?

Another analysis that could be done in this case would be a thermal and gas emission monitoring. Thermal monitoring could be done with NASA FIRMS website, as it was done with Copernicus data, obtaining data from the Moderate resolution Imaging Spectroradiometer in NASA's satellites, for example. Gas emission monitoring could be done with Sentinel-5P satellite, using the TROPOMI instrument, in order to monitorize the SO_2 emissions.

Chapter 5

Land Cover Prediction

5.1 Affected and Changed Areas

For analysing the affected area, land cover classification is applied to the data acquired from the time after the outbreak. We trained two classification models to predict the type of cover of the affected area. For details on both models, documentation of performance is provided in the appendix. The unaffected land cover is shown in Figure 5.1.

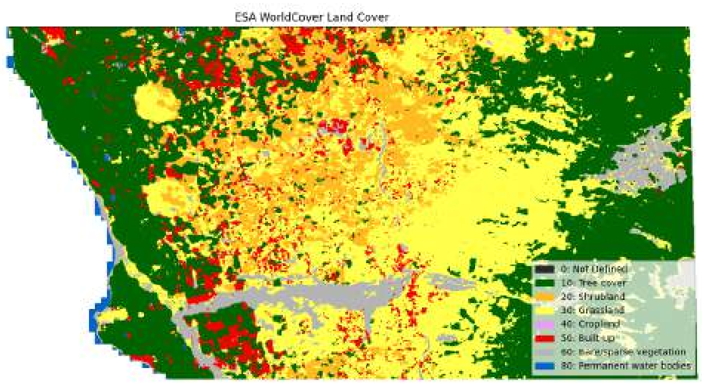

Figure 5.1: Land Cover before the outbreak

Figure 5.2 shows the impact of the outbreak. These land cover classifications are inferred by the previously trained models.

5.2 What is the final area you define as affected by the disaster? Which part would you consider the most severely impacted, and why?

The area affected by the volcanic eruption is primarily concentrated around the central region of the map, especially where we see much bare/sparse vegetation. In the original land cover map, this region was mainly classified as cropland, grassland, and built-up areas. indicating a severe transformation of the landscape. Interestingly, the crater of the volcano

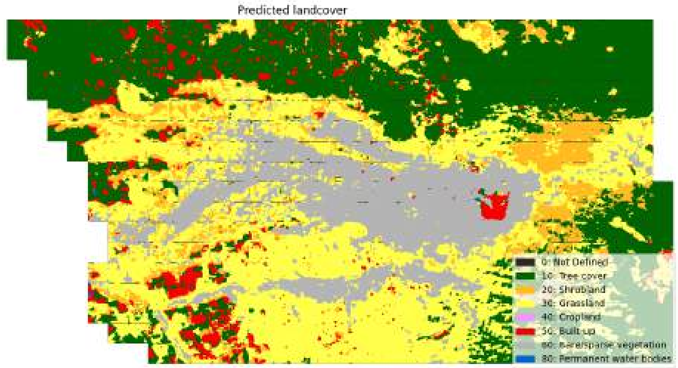

Figure 5.2: Land cover after outbreak according to simple CNN model

is classified now as built-up. The most severely impacted zone is the western section of the eruption site, where former vegetation and infrastructure were completely lost. The affected land is now either covered by lava, ash, or damaged infrastructure and dirt.

5.3 Is there anything notable or unique in the affected area?

Yes, there are notable features in the affected area. One key observation is the disappearance of built-up areas (except of the crater). All infrastructure in this region is most probably destroyed. The significant increase in bare /sparse vegetation. These changes can narrow down the core impact zone.

5.4 What considerations or recommendations should be proposed?

- Conduct a detailed risk assessment and zoning analysis in the affected region to restrict future development in high-risk zones, if there is a risk of it happening again.
- Use satellite-based monitoring with higher temporal resolution to track vegetation regrowth, infrastructural rebuild.
- Provide support for recovery planning, particularly in regions where cropland and infrastructure have been lost.
- Improve land cover models with disaster-specific training data to handle extreme and rapidly changing environments more effectively (which is important, as data of such disasters are rare).

Bibliography

[1] E. S. Agency, “La Palma volcano: How satellites help us monitor eruptions,” 2021. Accessed: 2025-05-25.

[2] S. Sennert, “Report on la palma (spain) — october 2021,” tech. rep., Smithsonian Institution, 2021.

[3] S. Sennert, “Report on la palma (spain) — 8 december-14 december 2021,” tech. rep., Smithsonian Institution, 2021.

[4] C. Programme, “The observer: Copernicus eyes the la palma eruption,” 2021.

[5] O. Ronneberger, P. Fischer, and T. Brox, “U-net: Convolutional networks for biomedical image segmentation,” in *Medical image computing and computer-assisted intervention–MICCAI 2015: 18th international conference, Munich, Germany, October 5-9, 2015, proceedings, part III 18*, pp. 234–241, Springer, 2015.

Chapter 6

Appendix

The appendix contains all additional data and images which were used in the analysis.

6.1 Visualization of Indices

Below, the computed indexes are displayed for each acquisition.

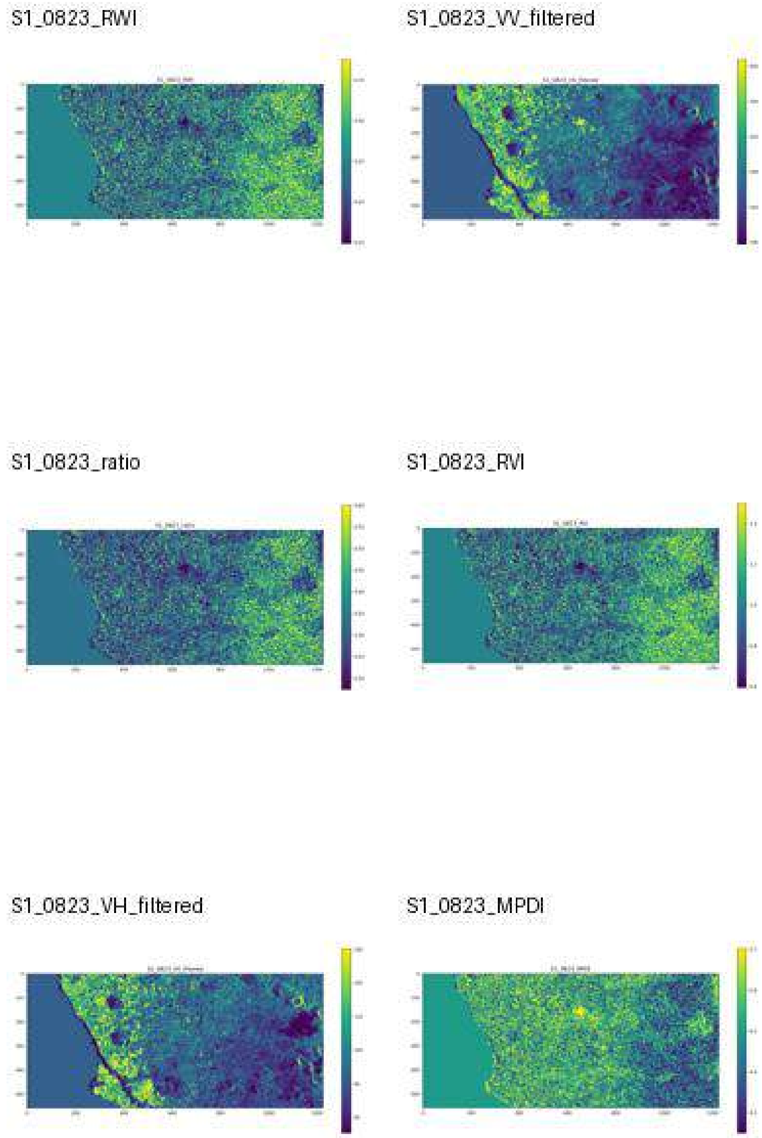

Figure 6.1: S1 indices (08232021)

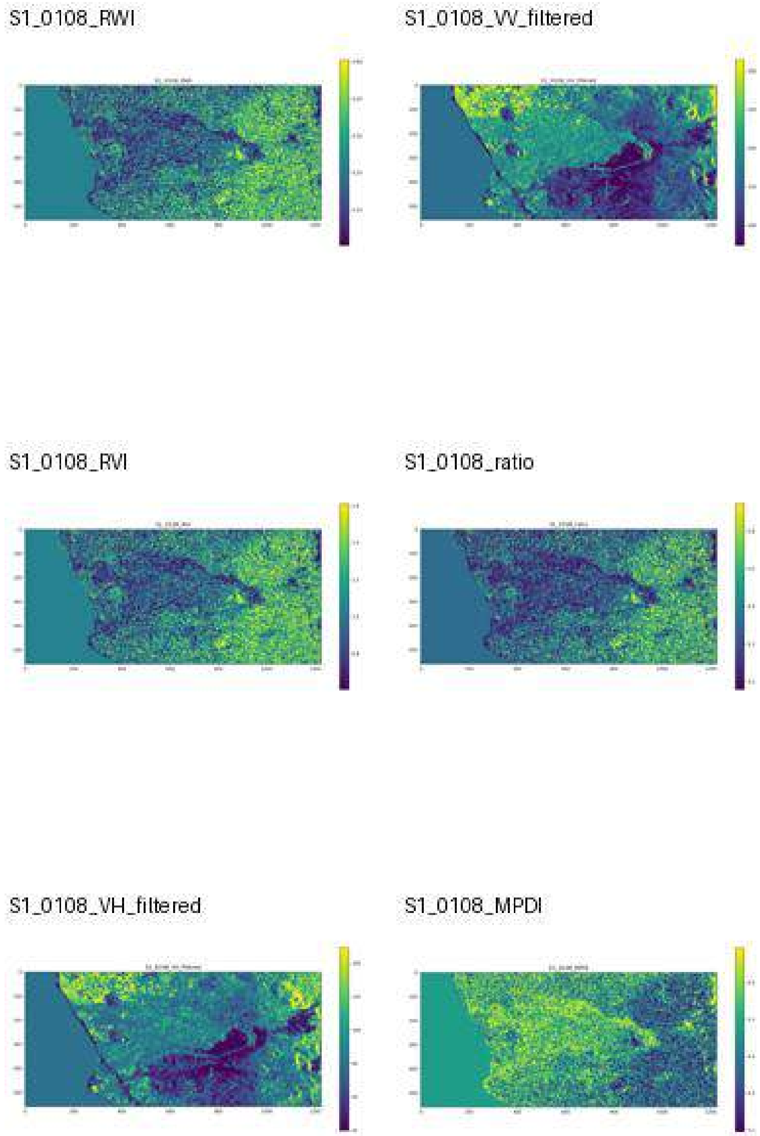

Figure 6.2: S1 indices (01082022)

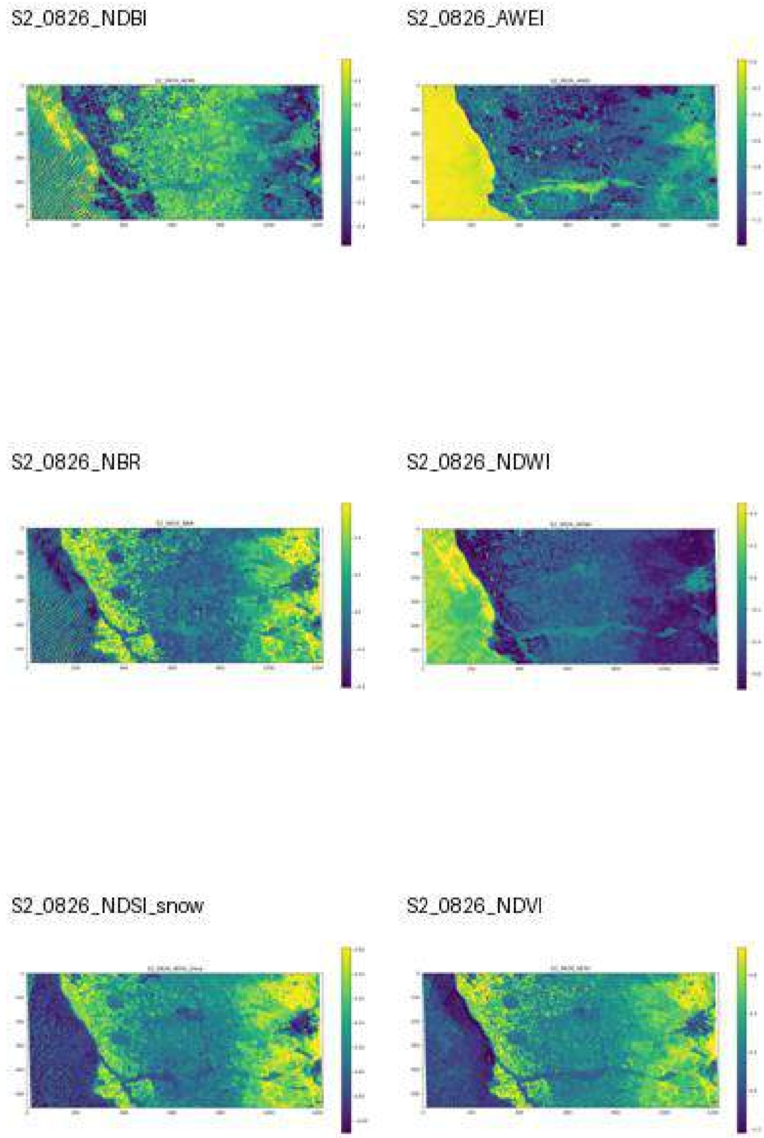

Figure 6.3: S2 indices (08262021)

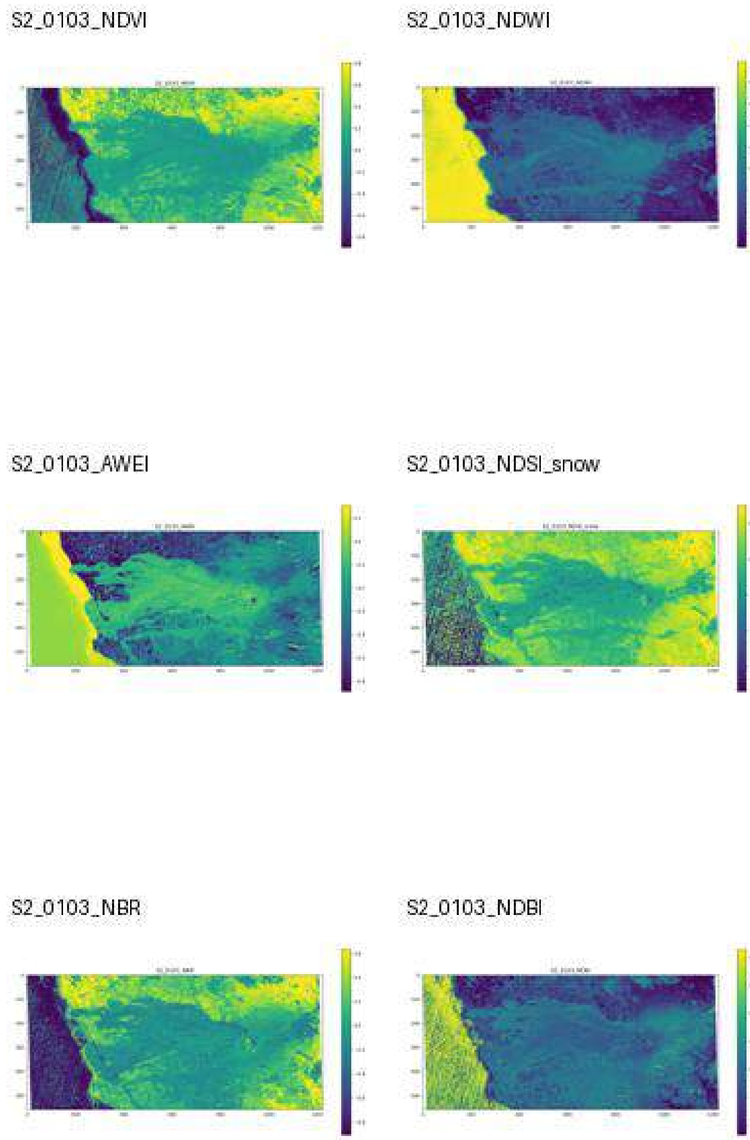

Figure 6.4: S2 indices (01032022)

Paired Plots

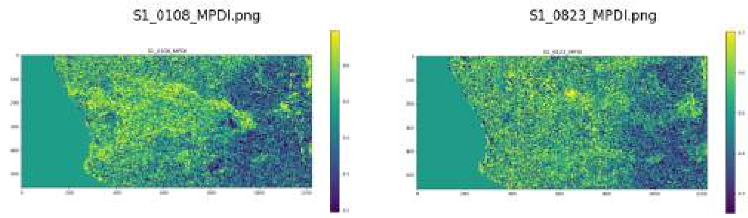

Figure 6.5: paired_S1_MPDI.png

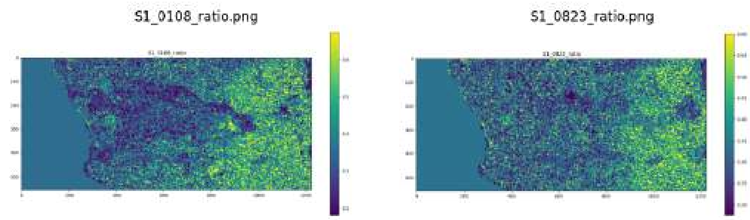

Figure 6.6: paired_S1_ratio.png

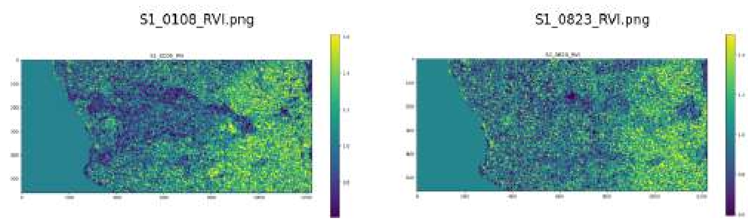

Figure 6.7: paired_S1_RVI.png

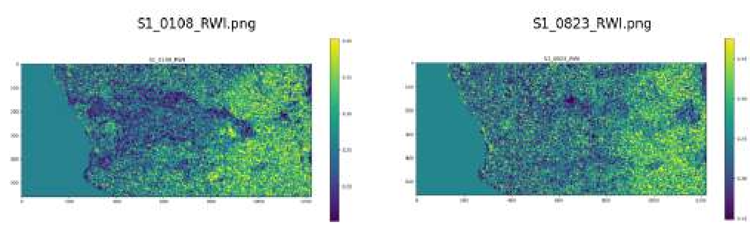

Figure 6.8: paired_S1_RWI.png

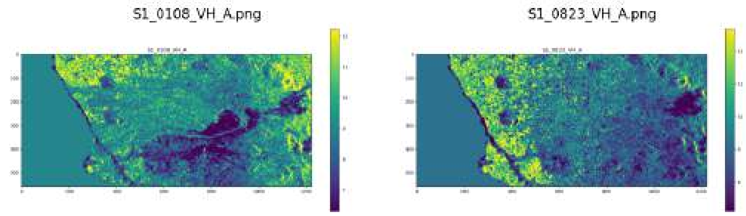

Figure 6.9: paired_S1_VH_A.png

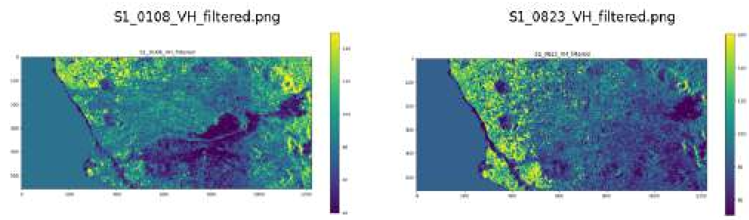

Figure 6.10: paired_S1_VH_filtered.png

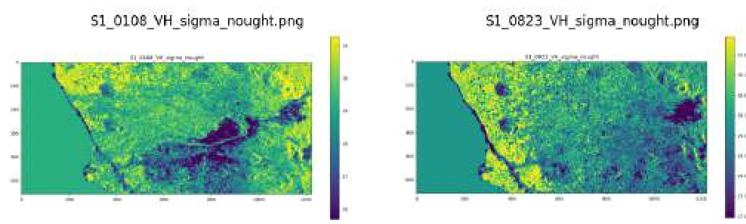

Figure 6.11: paired_S1_VH_sigma_nought.png

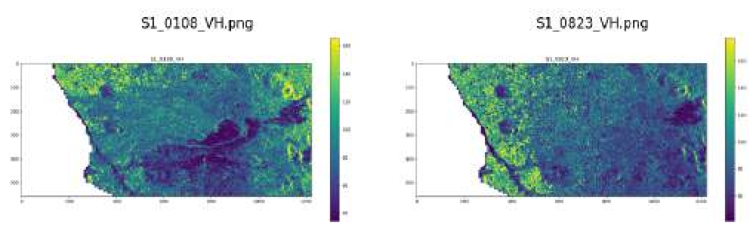

Figure 6.12: paired_S1_VH.png

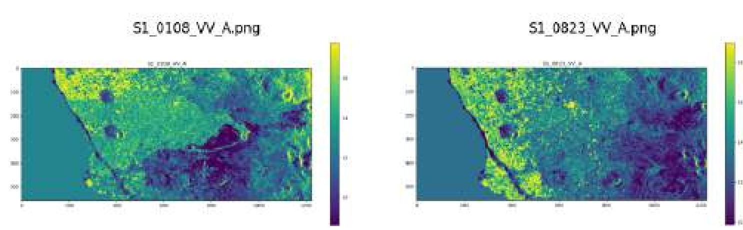

Figure 6.13: paired_S1_VV_A.png

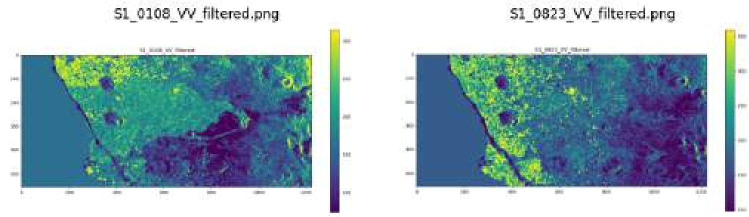

Figure 6.14: paired_S1_VV_filtered.png

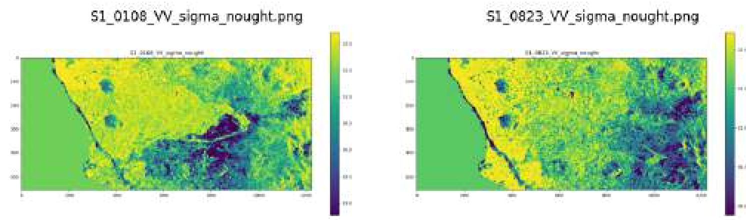

Figure 6.15: paired_S1_VV_sigma_nought.png

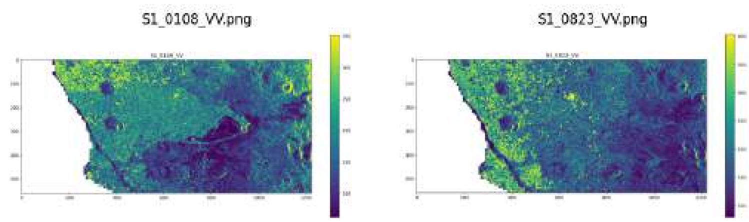

Figure 6.16: paired_S1_VV.png

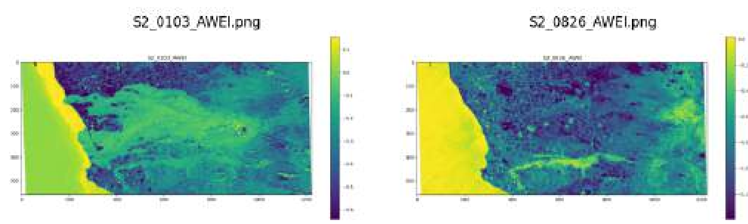

Figure 6.17: paired_S2_AWEI.png

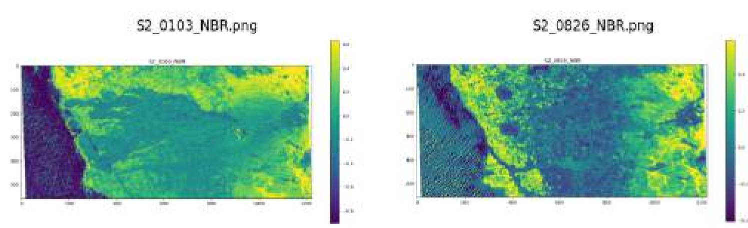

Figure 6.18: paired_S2_NBR.png

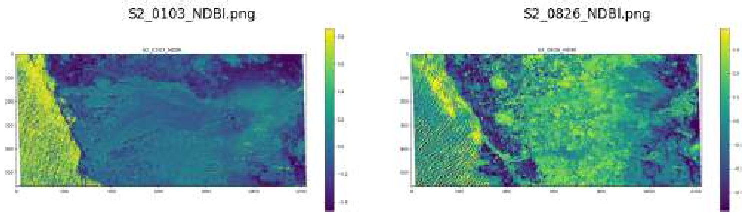

Figure 6.19: paired_S2_NDBI.png

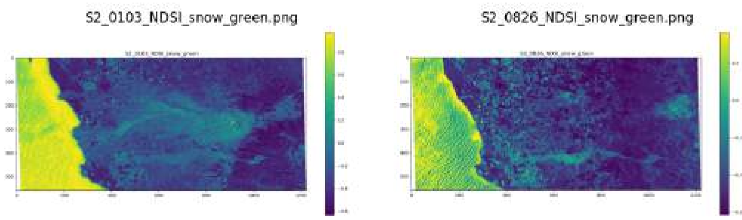

Figure 6.20: paired_S2_NDSI_snow_green.png

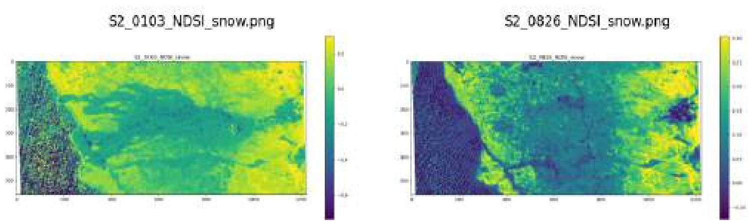

Figure 6.21: paired_S2_NDSI_snow.png

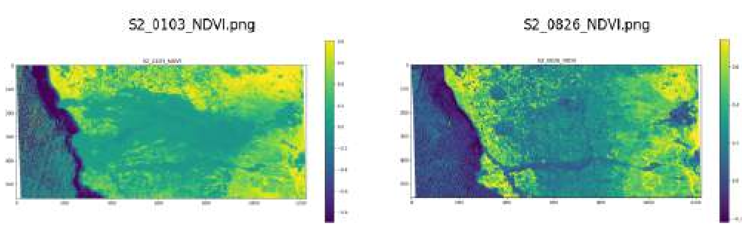

Figure 6.22: paired_S2_NDVI.png

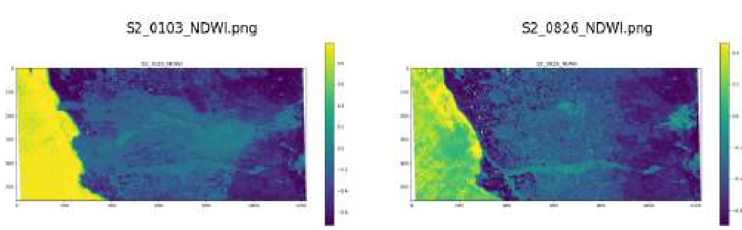

Figure 6.23: paired_S2_NDWI.png

6.2 Land Cover Classification

For classification, convolutional neural networks have been used, as they are good at extracting visual features from images. Two models with different types of architecture have been applied. One model uses a simple architecture consisting of a few convolutional layers. The second model's architecture is inspired by the famous U-net [5]. Figure 6.25 shows the architecture. The models have been trained on all data acquired before the outbreak. The inference results on the validation set can be seen in Table 6.1 and Table 6.1. The model's inference on the training data can be seen here, and the difference.

Class	**Precision**	**Recall**	**F1-score**	**Support**
Not Defined	0.149	0.825	0.253	1 056
Tree cover	0.924	0.796	0.855	213 163
Shrubland	0.562	0.784	0.654	62 210
Grassland	0.794	0.624	0.699	175 946
Cropland	0.445	0.352	0.393	219
Built-up	0.415	0.815	0.550	32 519
Bare/sparse vegetation	0.733	0.878	0.799	31 761
Permanent water bodies	0.676	0.918	0.779	758
Accuracy				517 632
Macro avg	0.587	0.749	0.623	517 632
Weighted avg	0.790	0.742	0.754	517 632

Table 6.1: Classification report for land cover prediction, CNN

Class	**Precision**	**Recall**	**F1-score**	**Support**
Not Defined	0.595	0.762	0.668	1 056
Tree cover	0.930	0.866	0.897	213 163
Shrubland	0.731	0.878	0.798	62 210
Grassland	0.875	0.766	0.816	175 946
Cropland	0.814	0.320	0.459	219
Built-up	0.533	0.855	0.657	32 519
Bare/sparse vegetation	0.811	0.918	0.861	31 761
Permanent water bodies	0.754	0.891	0.817	758
Accuracy				517 632
Macro avg	0.755	0.782	0.747	517 632
Weighted avg	0.854	0.835	0.839	517 632

Table 6.2: Classification report for land cover prediction, Unet

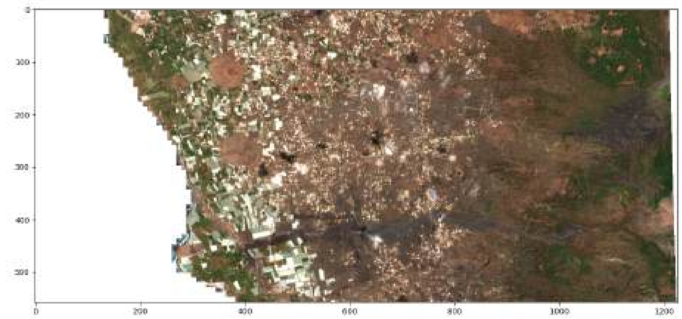

Figure 6.24: RGB image of training data

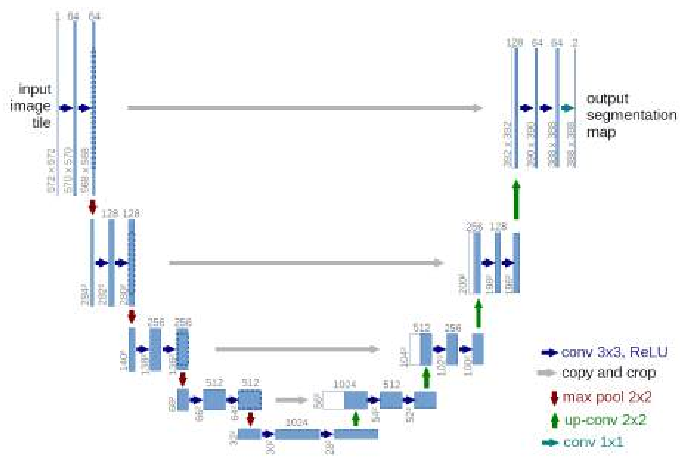

Figure 6.25: U-net Architecture

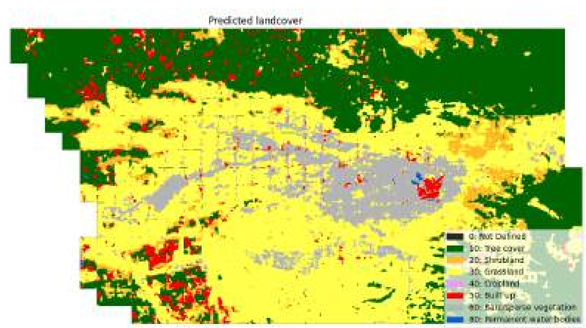

Figure 6.26: Land cover after outbreak according to U-net model